The Journal of Chemical Physics

Photoelectron spectra of 2-thiouracil, 4-thiouracil, and 2,4-dithiouracil

Cite as: J. Chem. Phys. **144**, 074303 (2016); https://doi.org/10.1063/1.4941948
Submitted: 09 December 2015 . Accepted: 02 February 2016 . Published Online: 17 February 2016

Matthias Ruckenbauer, Sebastian Mai, Philipp Marquetand, and Leticia González

View Online Export Citation CrossMark

ARTICLES YOU MAY BE INTERESTED IN

Communication: The dark singlet state as a doorway state in the ultrafast and efficient intersystem crossing dynamics in 2-thiothymine and 2-thiouracil
The Journal of Chemical Physics **140**, 071101 (2014); https://doi.org/10.1063/1.4866447

State-specific heavy-atom effect on intersystem crossing processes in 2-thiothymine: A potential photodynamic therapy photosensitizer
The Journal of Chemical Physics **138**, 044315 (2013); https://doi.org/10.1063/1.4776261

Short-time dynamics of 2-thiouracil in the light absorbing $S_2(\pi\pi^*)$ state
The Journal of Chemical Physics **143**, 175103 (2015); https://doi.org/10.1063/1.4935047

The Journal of Chemical Physics 2018 EDITORS' CHOICE READ NOW!

AIP Publishing

© 2016 AIP Publishing LLC.

Photoelectron spectra of 2-thiouracil, 4-thiouracil, and 2,4-dithiouracil

Matthias Ruckenbauer, Sebastian Mai, Philipp Marquetand,[a] and Leticia González[b]
Institute of Theoretical Chemistry, University of Vienna, Währinger Straße 17, 1090 Vienna, Austria

(Received 9 December 2015; accepted 2 February 2016; published online 17 February 2016)

Ground- and excited-state UV photoelectron spectra of thiouracils (2-thiouracil, 4-thiouracil, and 2,4-dithiouracil) have been simulated using multireference configuration interaction calculations and Dyson norms as a measure for the photoionization intensity. Except for a constant shift, the calculated spectrum of 2-thiouracil agrees very well with experiment, while no experimental spectra are available for the two other compounds. For all three molecules, the photoelectron spectra show distinct bands due to ionization of the sulphur and oxygen lone pairs and the pyrimidine π system. The excited-state photoelectron spectra of 2-thiouracil show bands at much lower energies than in the ground state spectrum, allowing to monitor the excited-state population in time-resolved UV photoelectron spectroscopy experiments. However, the results also reveal that single-photon ionization probe schemes alone will not allow monitoring all photodynamic processes existing in 2-thiouracil. Especially, due to overlapping bands of singlet and triplet states the clear observation of intersystem crossing will be hampered. © *2016 AIP Publishing LLC.* [http://dx.doi.org/10.1063/1.4941948]

I. INTRODUCTION

Thionucleobases, which are nucleobase analogues where one or more oxygen atoms have been substituted by sulphur, play an important role in molecular biology and pharmacology. They are, e.g., contained in natural t-RNA[1,2] and, given their structural similarity to canonical nucleobases, they can be used as fluorescent probes in DNA and RNA,[3,4] as well as for pharmaceutical purposes such as photosensitizers for photodynamic therapy[5,6] or antithyroid drugs.[7] Besides their occurrence in biological environments and wide applicability, thiobases have received a lot of attention due to their remarkably different photophysics in comparison to canonical nucleobases. Despite their similar structure, the presence of a thiocarbonyl group results in a red-shift of the UV absorption spectrum and an increase of intersystem crossing.[8–10] These differences have prompted a large number of studies with focus on their electronic structure[11–14] and excited-state dynamics, both from the theoretical[15] and experimental points of view, in particular by means of transient absorption spectroscopy.[9,10,16–19]

Among thiobases, the thiouracils, 2-thiouracil (2TU), 4-thiouracil (4TU), and 2,4-dithiouracil (DTU), are particularly interesting. Under experimental conditions, all three compounds exist only in their oxothione or dithione tautomeric form[20] (see Fig. 1). The UV absorption spectra[10,16,21–23] and photodeactivation mechanism[13,16,18,19] of 2TU have been analysed extensively; the absorption spectrum is slightly red-shifted compared to uracil and shows signs of a low-lying dark $n\pi^*$ state.[8] The UV absorption spectra of 4TU and DTU are considerably red-shifted compared to 2TU,[9,19] but their general excited-state behaviour appears to be not much different from the one of 2TU: all three molecules show sub-picosecond intersystem crossing after excitation to the first absorption band.[19] In contrast to the UV absorption spectra, not much has been reported on the photoelectron spectra of thiouracils. The main interest in this respect has been laid on the anions of these compounds,[24,25] because ionizing radiation creates anions on the way to single and double strand breaks in DNA. A single study on the tautomerism of 2TU and its methyl derivates[26] contains a static He(I) photoelectron spectrum of neutral 2TU.

Also, to our knowledge, no time-resolved photoelectron spectroscopy (TRPES)[27] has been reported for these molecules, even though this methodology has been extensively applied to study the excited-state dynamics of the canonical nucleobases[28–30] (see, e.g., Ref. 31 for a list of these experiments) and a small number of nucleobase analogous.[32,33] TRPES has a number of advantages with respect to other spectroscopic techniques, e.g., it allows to study the excited-state dynamics in the gas phase, while methods like transient absorption spectroscopy usually measure solvated compounds. Furthermore, due to very different selection rules for photoionization compared to absorption, in TRPES it is possible to probe dark states, which is very useful to elucidate the photophysical intermediates of these compounds. Such knowledge can be particularly relevant for thiouracils, helping to promote the use and eventual functionalization of thiobases with phototherapeutic aims.

With this in mind, in this paper we report theoretical UV-photoelectron spectra of 2TU, 4TU, and DTU from the ground state equilibrium geometries. We describe the character of the various ionization source orbitals and how thio-substitution influences the number, intensity, and position of the bands in the low-energy spectra. For 2TU, we also explore the photoelectron spectra from the neutral excited states at the Frank-Condon region as well as around the

[a]Electronic mail: philipp.marquetand@univie.ac.at
[b]Electronic mail: leticia.gonzalez@univie.ac.at

 © 2016 AIP Publishing LLC

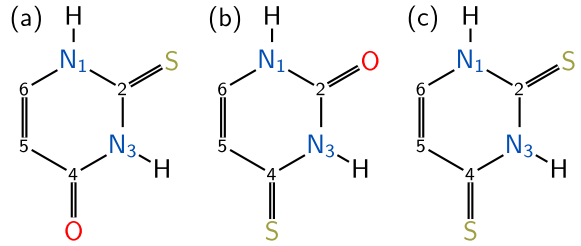

FIG. 1. Structures of (a) 2-thiouracil (2TU), (b) 4-thiouracil (4TU), and (c) 2,4-dithiouracil (DTU), with numbering of the ring atoms. Hydrogen atoms attached to carbons are omitted.

stationary points on the potential energy surface of the lowest excited singlet and triplet states, complementing our recent study[13] on the relaxation and intersystem crossing mechanism after UV irradiation of this molecule. While we do not report time-resolved photoelectron spectra here, the spectra at the stationary points indicate that single-photon UV-TRPES alone probably cannot discern the different deactivation pathways, in particular intersystem crossing, of photoexcited 2TU and should be complemented by some other method to probe the excited-state population.

II. METHODS

A. Theory

An efficient way to calculate static ground or excited-state UV-photoelectron spectra is to employ Dyson norms as a measure of the ionization intensities. This approach neglects the explicit treatment of the continuum wavefunction of the outbound electron and the calculation of the transition dipole moment matrix elements. While an accurate treatment of these ingredients is possible, e.g., as done in Ref. 34, this is computationally very expensive and different approximations strive to reduce this high cost.[35] Luckily, in the case of single-photon ionization, the norms of Dyson orbitals have been shown to be a good approximation for relative ionization probabilities.[34,36–38] An excellent introduction to the description of photoionization using Dyson orbitals can be found in Refs. 34, 39, and 40, so here we only provide a brief overview.

In the following, we describe transitions from a neutral source state i to an ionic state α as the ionization channel $i \to \alpha$. The corresponding Dyson orbital $\left|\phi^{\mathrm{D}}_{i,\alpha}\right\rangle$, which can be thought of as the wavefunction of the electron to be detached, is defined as

$$\left|\phi^{\mathrm{D}}_{i,\alpha}\right\rangle := \sqrt{n}\left\langle \Theta^{(n-1)}_{\mathrm{ion},\alpha} \middle| \Psi^{(n)}_{\mathrm{src},i} \right\rangle_{(n-1)}, \tag{1}$$

with the n-electron source wavefunction $\left|\Psi^{(n)}_{\mathrm{src},i}\right\rangle$, as well as the $(n-1)$-electron ionic wavefunction $\left|\Theta^{(n-1)}_{\mathrm{ion},\alpha}\right\rangle$. The subscript $(n-1)$ of the bracket indicates integration over $n-1$ electrons. As a measure for the relative ionization yield $W_{i,\alpha}$, we use an expression analogous to the oscillator strength, where the Dyson norm is scaled with the energy difference $\Delta E_{i,\alpha}$ between the n-electron source state i and the $(n-1)$-electron state α,

$$W_{i,\alpha} \propto \Delta E_{i,\alpha} \left\langle \phi^{\mathrm{D}}_{i,\alpha} \middle| \phi^{\mathrm{D}}_{i,\alpha} \right\rangle. \tag{2}$$

The oscillator strength in general for a transition from a state i to a state u is $f_{iu} \sim \Delta E_{iu} |\langle u|\hat{\mu}|i\rangle|^2$ with the energy difference ΔE_{iu} between the states and the dipole operator $\hat{\mu}$.[41] Equation (2) is analogous since the dipole moment operator $\hat{\mu}$ is approximated as a constant of value one and we do not explicitly consider the continuum wavefunction of the free electron $\left|\chi^{\vec{k}}_{\alpha}\right\rangle$.[34] Note that the sum of all possible oscillator strengths originating from one state is equal to the number of excitable electrons z according to the f-sum rule: $\sum_j f_{ij} + \int_0^\infty f_{i\varepsilon} \mathrm{d}\varepsilon = z$, where ij indicate all possible transitions from state i within the neutral molecule and $i\varepsilon$ stands for transitions to the continuum.[41]

In the case of wavefunctions of the configuration interaction (CI) type expanded in Slater determinants with orthonormal spin orbitals $\theta_{a,r}$ and $\psi_{b,s}$,

$$\begin{aligned}
\left|\Theta^{(n-1)}_{\mathrm{ion},\alpha}\right\rangle &= \sum_a c_{\mathrm{ion},\alpha,a} \left|\Theta^{(n-1)}_{\mathrm{ion},\alpha,a}\right\rangle, \\
\left|\Theta^{(n-1)}_{\mathrm{ion},\alpha,a}\right\rangle &= \frac{1}{\sqrt{(n-1)!}} \left|\theta_{a,1} \ldots \theta_{a,r} \ldots \theta_{a,(n-1)}\right\rangle, \\
\left|\Psi^{(n)}_{\mathrm{src},i}\right\rangle &= \sum_b c_{\mathrm{src},i,b} \left|\Psi^{(n)}_{\mathrm{src},i,b}\right\rangle, \\
\left|\Psi^{(n)}_{\mathrm{src},i,b}\right\rangle &= \frac{1}{\sqrt{n!}} \left|\psi_{b,1} \ldots \psi_{b,s} \ldots \psi_{b,n}\right\rangle,
\end{aligned}$$

the total Dyson orbital is the sum of the overlaps of all Slater determinant pairs (indices a, b) weighted with the product of their CI coefficients

$$\left|\phi^{\mathrm{D}}_{i,\alpha}\right\rangle_{\mathrm{CI}} = \sum_a \sum_b c^*_{\mathrm{ion},\alpha,a} c_{\mathrm{src},i,b} \left|\phi^{\mathrm{D}}_{i,\alpha}\right\rangle_{a,b}. \tag{3}$$

To this end, the contribution of one Slater determinant pair $\left\langle \Theta^{(n-1)}_{\mathrm{ion},\alpha,a} \right|$ and $\left|\Psi^{(n)}_{\mathrm{src},i,b}\right\rangle$ can be rewritten in terms of the molecular spin-orbitals of the source wavefunction, $\left|\psi_{b,s}\right\rangle$, and the annihilation operator, $\hat{\mathbf{a}}_s$, for the sth occupied source spin-space orbital, $\left|\psi_{b,s}\right\rangle$,

$$\begin{aligned}
\left|\phi^{\mathrm{D}}_{\alpha}\right\rangle_{a,b} &= \sqrt{n}\left\langle \Theta^{(n-1)}_{\mathrm{ion},\alpha,a} \middle| \Psi^{(n)}_{\mathrm{src},i,b} \right\rangle_{(n-1)} \\
&= \sqrt{n} \sum_s^{\mathrm{occ_{src}}} \left\langle \Theta^{(n-1)}_{\mathrm{ion},\alpha,a} \middle| \hat{\mathbf{a}}_s \middle| \Psi^{(n)}_{\mathrm{src},i,b} \right\rangle_{(n-1)} \left|\psi_{b,s}\right\rangle.
\end{aligned} \tag{4}$$

The overlap $\left\langle \Theta^{(n-1)}_{\mathrm{ion},\alpha,a} \middle| \hat{\mathbf{a}}_s \middle| \Psi^{(n)}_{\mathrm{src},i,b} \right\rangle_{(n-1)}$ can be then obtained as a matrix determinant over appropriate molecular orbital overlap integrals.

B. Computational details

The source and ionic wavefunctions have been calculated with the quantum-chemistry package Columbus 7.0[42,43] using atomic integrals (including Douglas-Kroll-Hess scalar relativistic integrals[44]) from Molcas 8.0.[45] The cc-pVDZ basis set[46,47] was used in all calculations. Neutral and ionic wavefunctions were computed on the multireference configuration interaction with single excitations (MRCIS) level of theory using orbitals taken from the preceding complete active space self-consistent field (CASSCF)

calculations. The active space comprised 14 valence electrons (13 for doublets) in 10 orbitals. To describe ionization from the singlet states, state-averaging (SA) with equal weights has been performed using 4 states for the neutral singlet and 10 states for the ionized doublet wavefunctions, denoted as SA(4S) and SA(10D), respectively. To describe ionization from the triplet states, the neutral and ionized states employed a SA(4S+4T) and SA(10D+10Q) averaging protocol, respectively. See the supplementary material for the active space orbitals.[48]

In the MRCIS calculation, the active orbitals of the preceding CASSCF have been used as reference space, restricting the references to configurations with at most two electrons in the three antibonding π^* orbitals. The full MRCIS wavefunctions contained these references, plus all single excitations from occupied to active, occupied to virtual, and active to virtual orbitals. Inner shell orbitals ($1s$ of C,N,O,S and $2s/2p$ of S) were not correlated; these are 12 orbitals for 2TU and 4TU and 16 orbitals for DTU (due to the second sulphur atom). A total of 12 doublet and quartet (if applicable) states were computed on the MRCIS level of theory. This level of theory cannot accurately describe singlet and triplet excitation energies due to a deficiency of dynamic correlation (see below). However, having all important ionization source orbitals in the reference space ensures an adequate description of the lower ionized states.

Using the so-obtained wavefunctions, Dyson norms have been calculated to estimate photoionization probabilities. To reduce the computational cost, the CI vectors were truncated by removing the configuration state functions with the smallest absolute coefficients until the remaining wavefunction had a norm of 0.97.[49] A careful inspection showed that this procedure strongly reduces the computational costs of the Dyson norms without significant deterioration of the results.

Finally, photoelectron spectra have been calculated from the S_0 minimum and, in the case of 2TU also from the S_1 and T_1 minima, optimized at the MRCIS level of theory specified above (see the supplementary material for the optimized geometries[48]). In order to simulate vibrational broadening, for each compound 200 geometries were sampled randomly from a Wigner distribution based on frequencies obtained at the MRCIS level of theory. For each geometry, the Dyson norms for all applicable pairs of states were computed using the molecular orbital coefficients and CI vectors from the corresponding quantum-chemistry calculations. Spectra were calculated as a sum over Gaussians centered at the excitation energies and height proportional to W in Equation (2). A full width at half-maximum of 0.2 eV was chosen for the purpose of obtaining a smoothed spectrum from the calculated number of geometries. The photoelectron spectrum of the ground state of 2TU was normalized to a maximum signal of one, and the same normalization factor was then used for all other spectra. (Note that all spectra were calculated with the same number of geometries and the same full width at half-maximum.) The generation of photoelectron spectra has been performed using tools from the development version of the Sharc molecular dynamics suite.[50–52]

III. RESULTS AND DISCUSSION

A. Assessment of vertical binding energies

The binding energies calculated in this work are based on a Δ-CI approach, i.e., we calculate independently the energies of neutral and ionic wavefunctions and their difference is the binding energy. The Δ-CI approach allows to describe all ionic states independent of Koopmans-type assumptions, i.e., orbital relaxation and correlation effects are automatically included for all ionic states (including "shake-up" states with simultaneous electron removal and excitation of another electron). Unfortunately, with a Δ-CI approach it is often difficult to balance the electron correlation treatment between neutral and ionic wavefunctions[53] (e.g., for 2TU, neutral CI functions incorporated 900.000 configuration state functions, whereas ionic wavefunctions contained about 5 million configuration state functions). Therefore, we assess the quality of the MRCIS binding energies by comparing to MS-CASPT2 calculations (multi-state complete-active space perturbation theory). The latter method is—to a large degree—size-extensive, thus balances better electronic correlation and yields more accurate binding energies.

In particular, we performed MS-CASPT2(n,10)/cc-pVTZ (n = 14 for neutral and 13 for ionic wavefunctions) calculations for 2TU and compared the binding energies to the corresponding values from the MRCIS method outlined above. Figure 2 shows a scatter plot of the binding energies at MRCIS and MS-CASPT2 levels of theory. The supplementary material[48] contains the numerical data and further computational details for the MS-CASPT2 calculation. The figure shows that the MRCIS binding energies are systematically lower than the MS-CASPT2 energies. However, the order of states is the same for both methods, and the error is approximately constant for all states. For the first four states, the energy shift is about −1.5 eV, whereas for the next six states it is about −1.2 eV. As low-lying states are usually better described in MRCIS than high-lying ones, we deem the wavefunction quality of D_{0-3} better than the quality of D_{4-11}. Fortunately, these deviations are acceptable for our current goal, i.e., simulating vibrationally broadened

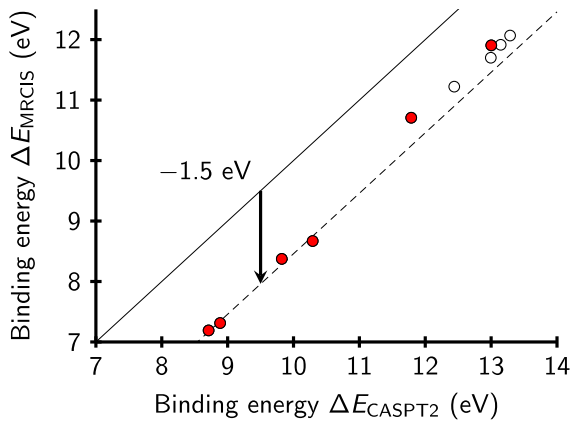

FIG. 2. Scatter plot of the MRCIS and MS-CASPT2 binding energies of 2TU. Filled dots refer to states with large Dyson norms (>0.1) and open rings to states with small Dyson norms. The solid line is the identity line, the dashed line indicates a linear fit of the first four points.

photoelectron spectra. Since it is apparent that a constant shift is necessary, we calibrate this shift from the experimental photoelectron spectrum of 2TU.

B. Photoelectron spectra of 2TU, 4TU, and DTU

The experimental photoelectron spectrum of 2TU, taken from Ref. 26, is shown in Figure 3, together with our computed spectrum for the S_0 as source state. We correct the systematic energy shift mentioned above by introducing a +1.7 eV off-set to the computed spectrum, as indicated in the figure. As explained above, this off-set originates from the lack of size extensivity[54] of MRCIS and the difference in the number of correlated electrons in neutral and ionized wavefunctions. As expected from the comparison to MS-CASPT2, the peak separations and relative peak heights in the simulated spectrum agree well with the experimental data, particularly at low energies, showing that the method predicts the energetic spacing of the ionic states and the relative intensities correctly.

For higher binding energies, the experimental spectrum shows a very broad band starting at ≈11 eV, which could not be reproduced well by our calculations. We assume that this band originates either from ionization to higher-lying shake-up doublet states or from ionization from σ orbitals, both effects not well described by our simulation. An extension of the simulated energy range to higher doublet states with the present level of theory is not expected to yield better results because already in the present calculations the highest states (D_{9-11}) are strongly mixed and have large contributions of double excitations within the reference space. Since the description of higher-lying states would require a much more accurate electronic structure method, which is out of the scope of this paper, the discussions below focus on the lower part of the spectrum.

The simulated photoelectron spectra of the neutral ground states of all three compounds are presented in Figure 4, together with the contributing signals of the ionization channels (D_0-D_{11}). While 2TU and 4TU both show three groups of signals, the spectrum of DTU is characterized by only two bands. The band lowest in energy (≈8 eV–10 eV) is common to all three compounds but it is more intense in DTU than in the other two molecules due to the different composition of the bands. Only the D_0 and D_1 ionization

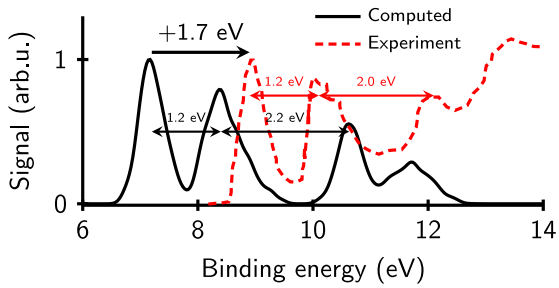

FIG. 3. Computed S_0-photoelectron spectrum for 2TU compared to the experimental spectrum from Katritzky *et al.*[26] Arrows indicate the band spacing and the shift of +1.7 eV needed to overlap the simulated spectrum with the experimental one.

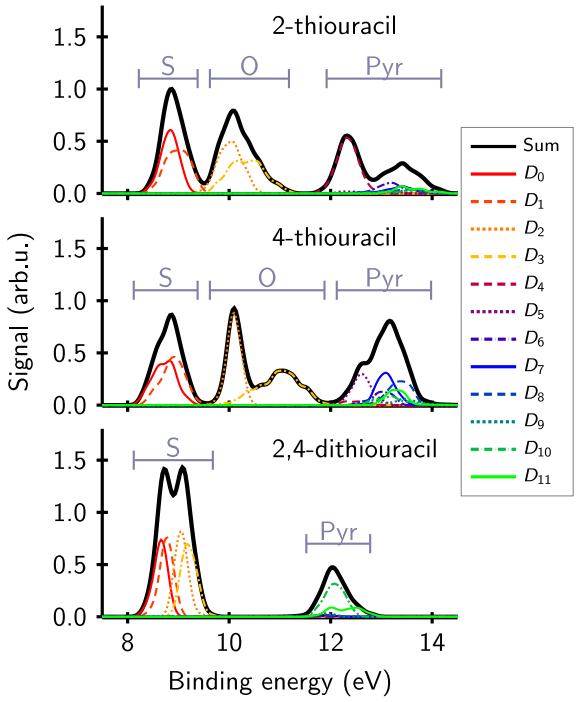

FIG. 4. Computed S_0-photoelectron spectra for 2TU, 4TU, and DTU with individual contributions of the first 12 ionization channels (D_0-D_{11}). "S," "O," and "Pyr" labels indicate predominant ionization from orbitals on sulphur, oxygen, and the pyrimidine ring, respectively. All spectra have been shifted by +1.7 eV (the off-set indicated in Figure 3).

channels contribute to the first band of 2TU and 4TU, whereas D_0-D_3 compose the first band of DTU. The next band higher in energy, centered around 10 eV is only present for 2TU and 4TU while there is no visible intensity for DTU. The shape of this band, which is different for 2TU compared to 4TU, is due to the different intensities and energies of the contributing D_2 and D_3 channels. The third band beyond 12 eV is different for each of the molecules.

An analysis of the ionization channels in terms of their corresponding Dyson orbitals, which describe the character of the departing electron's wavefunction, is very instructive to understand the differences between the spectra. Figure 5 shows all Dyson orbitals and their norm (if >0.1; see the supplementary material[48] for all Dyson norms) for the relevant ionization channels present in Figure 4. Note that the Dyson orbitals and norms shown are only exemplary, since they were taken from single-point calculations at the equilibrium geometry, while the spectra in Figure 4 include data from 200 single points per molecule. We also note that some Dyson norms are rather small, indicating that orbital relaxation and correlation effects are present and Koopmans' theorem is not valid for those ionization channels. However, our Δ-CI approach goes beyond Koopmans' theorem and can describe these ionization channels adequately.

As can be seen in Figure 5, the n and π orbitals of the sulphur atom are the dominant contributions to the Dyson orbitals of the $S_0 \rightarrow D_{0,1}$ ionizations in 2TU and 4TU, as well as of the $S_0 \rightarrow D_{0-3}$ ionizations in DTU. Accordingly, the first band of the three spectra is due to ionization from sulphur. The Dyson orbitals of the $S_0 \rightarrow D_{2,3}$ transitions in 2TU and 4TU correspond mostly to ionization from the n and π orbitals of

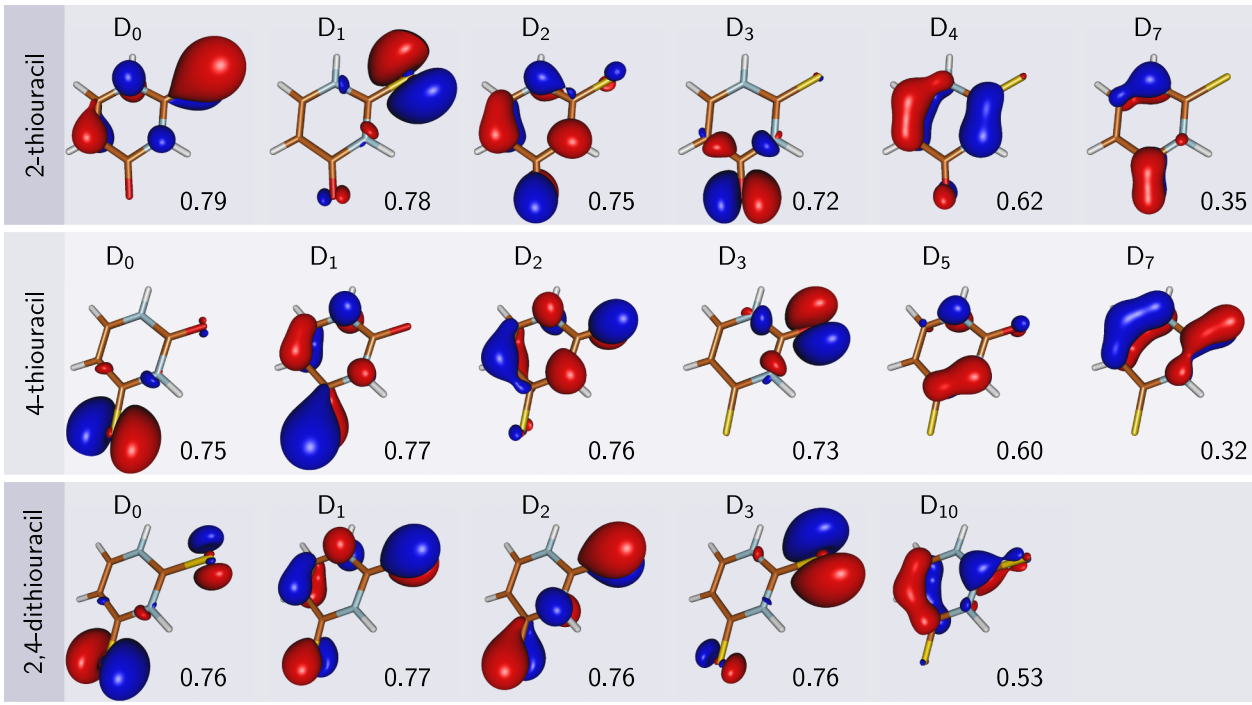

FIG. 5. Dyson orbitals and Dyson norms for the relevant ionization channels from the S_0 state of the three thiouracils. The orientation of the molecules is the same as in Figure 1.

oxygen. The different extent of mixing of the oxygen π orbital with pyrimidine π orbitals explains the differently shaped bands in 2TU and 4TU. Since there is no oxygen in DTU, it is apparent that this second band around 10 eV binding energy is missing in this compound. Finally, the signals in the high-energy range (>12 eV) contain the contributions of ionization from the π orbitals of the pyrimidine ring. The binding energy for electrons involved in a bond is naturally higher than for the lone pairs. The density of doublet states is very high in this energy region and many states show no significant intensity. For DTU, only the D_{10} yields substantial ionization probability. Hence, we assume that this band in the DTU spectrum is only partially described by our calculations.

The simulated spectra show that the three compounds, 2TU, 4TU, and DTU, could certainly be discriminated on the basis of their photoelectron spectra. DTU is clearly marked by the intensity of the sulphur-ionization band and the absence of an oxygen-ionization band. In contrast, 2TU and 4TU show distinctly different shapes of the band arising from ionization of oxygen-localized orbitals.

C. Excited-state photoelectron spectra of 2TU

Using the same set of geometries as for the 2TU S_0 photoelectron spectrum, the excited-state (source states S_1 and S_2) photoelectron spectra have been calculated (see Figure 6). The character of the neutral excited states at the equilibrium geometry is listed in Table I, together with vertical excitation energies and oscillator strengths, calculated at the MRCIS level of theory and compared to our recently published CASPT2 results.[13] Irrespective of the level of theory, the order of the states is the same and the S_1 state is an $n\pi^*$ excitation while the S_2 is a $\pi\pi^*$ state. In both states, an electron is excited from an orbital located at the sulphur atom and promoted to a π^* orbital on the pyrimidine ring. Quantitatively, one can see that the excitation energies are described too high at the MRCIS level of theory, more so for the $\pi\pi^*$ state. As this would lead to systematically too low binding energies in the simulation of photoelectron spectra with excited states as ionization source, an additional shift of +0.5 eV (towards higher binding energies) for the S_1 spectrum and +0.77 eV for the S_2 one was introduced.

Detachment of an electron which has been excited into an antibonding orbital (e.g., π^*) requires lower energy than

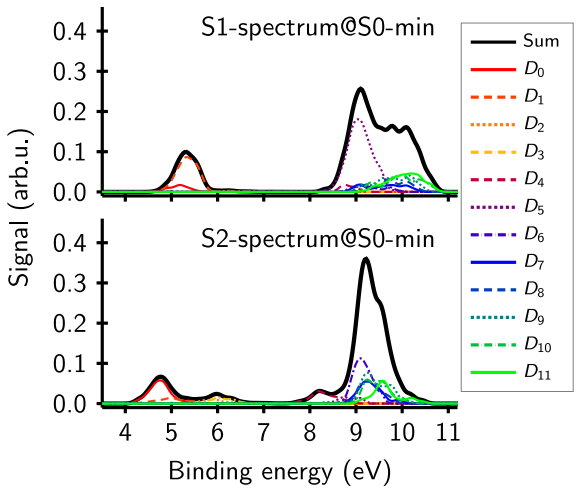

FIG. 6. Calculated S_1 ($n\pi^*$)- and S_2 ($\pi\pi^*$)-photoelectron spectra of 2TU including the contributions of all computed ionization channels. The spectra have been shifted by (1.7 + 0.5) eV and (1.7 + 0.77) eV for S_1 and S_2, respectively.

TABLE I. Calculated vertical excitation energies (eV) and oscillator strengths (in parentheses) of S_1 and S_2 and relative energies of S_1/T_1 minima of 2TU at the MRCIS and CASPT2 levels of theory, the latter taken from Ref. 13.

State	Geometry	This work	CASPT2(16,12)[13]
S_1 ($n_S\pi^*$)	S_0 min	4.27 (0.00)	3.77 (0.00)
S_2 ($\pi_S\pi^*$)	S_0 min	5.02 (0.29)	4.25 (0.35)
S_1 ($n_S\pi^*$)	S_1 min	3.79	3.45
T_1 ($\pi_S\pi^*$)	T_1 "boat" min	3.36	3.35
T_1 ($\pi_S\pi^*$)	T_1 "pyr." min	3.43	3.21

detachment of electrons in bonding orbitals. Consequently, the Dyson orbitals (Figure 7) for the first ionization channels ($S_1 \rightarrow D_1$ and $S_2 \rightarrow D_0$) are very similar to the π^* orbitals occupied in the S_1 and S_2 states. The second band arises mostly from ionization of the π orbital located at the $C_5{=}C_6$ bond. We note that the Dyson norms in Figure 7 are smaller than the ones in Figure 5, which shows that Koopmans theorem is not adequate for ionization from excited states.

The first band of each spectrum (Figure 6) is in the region of 4 eV–6 eV and thus more than 2 eV separated from the onset of the S_0 spectrum and from the next band in the excited-state spectra. Judging from the simulated spectra, it should be possible to obtain a clear signal from the lowest ionization channels of the excited singlet states without interference of the ground state signal using probe laser energies of 6 eV–8 eV. This allows for experimental studies using photoelectron spectroscopy to selectively track excited states. Furthermore, the spectra in Figure 6 show that S_1 and S_2 are distinguishable in the Frank-Condon region, but it is expected that during the dynamics after excitation their spectra will broaden and shift independently and hence might not be separable when moving away from the Franck-Condon point.

An important application of photoelectron spectroscopy in combination with pump-probe experiments is the ability to track different states and relaxation pathways in the excited-state dynamics. A recent exploration of the possible reaction pathways using static quantum-chemical calculations[13]

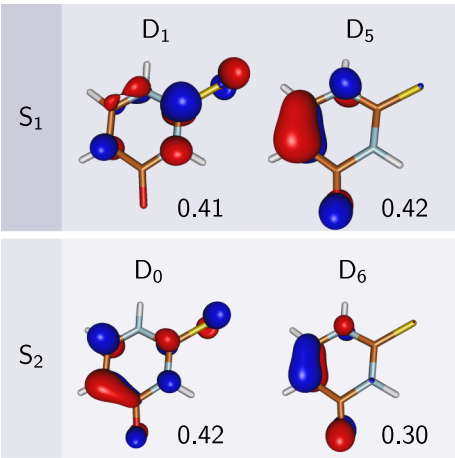

FIG. 7. Dyson orbitals and Dyson norms for the important low-energy ionization channels from the S_1 and S_2 states of 2TU.

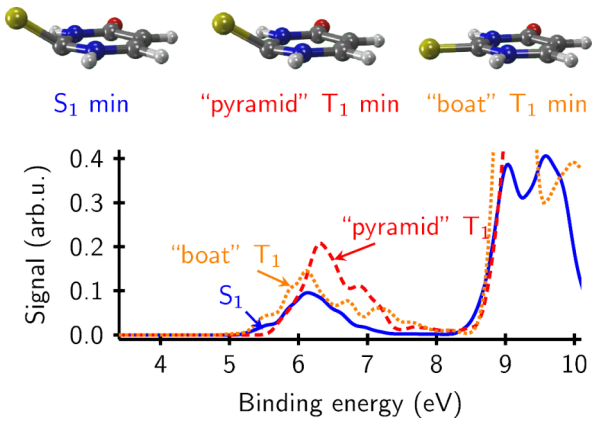

FIG. 8. Calculated photoelectron spectra of 2TU from the S_1 at the S_1 minimum and from the T_1 at the two T_1 minima (boat and pyramidalized conformations[13]). On the top, the minimum geometries are presented. The spectra have been shifted by +1.7 eV.

suggests that 2TU will, after electronic excitation to the S_2, quickly cross to the S_1 where it is trapped in a minimum with low chance to reach the crossing seam to the ground state. Instead, it is very likely that the system undergoes intersystem crossing into the energetically close T_2 state and from there internally converts into one of the two T_1 minima (named "boat" and "pyramidalized" in Ref. 13). An interesting question is to investigate whether it will be possible to gain insight into this intersystem crossing process of 2TU by TRPES. We therefore optimized the S_1 and both T_1 minima (geometries shown in Figure 8) and generated photoelectron spectra from these minima.

Table I collects the relative energies of these minima with respect to the equilibrium geometry at the MRCIS and MS-CASPT2 levels of theory. Despite the energetic order of the two T_1 minima being different with both methods, they are still very close in energy and no additional shift was applied. Figure 8 displays the three excited-state photoelectron spectra of 2TU. For each minimum, we obtain a weak band in the 5–8 eV energy range and an intense band above 8.5 eV, where the latter band is much more intense for the triplet state due to ionization to quartet states. The low-energy bands are quite similar and strongly overlapping and the high-energy band will likely be covered by ionization from the ground state. Hence, based on these spectra, we suggest that the S_1 and T_1 states cannot be discriminated by single-photon ionization using a probe laser in the suggested energy range of 6 eV–8 eV. Depending on the actual probe laser energy used, only part of the bands will contribute to the signal and hence a low intensity can be expected. Most importantly, the bands of the three spectra overlap strongly, and as can be seen, the small error in the energies of the neutral states due to MRCIS is not relevant. Based on these results, we predict that single-photon TRPES alone will not allow to track the population transfer from S_1 to T_1 in 2TU.

IV. CONCLUSIONS

The UV-photoelectron spectra of three thio-analogues of uracil, 2TU, 4TU, and DTU have been simulated using Dyson

norms as a measure for the relative ionization probabilities of the different ionization channels. In all three molecules, the respective first band of the photoelectron spectra is mainly due to ionization from the n and π orbitals on sulphur. For 2TU and 4TU, the second band corresponds to ionization from the n and π orbitals on oxygen, while for all three compounds the highest calculated band is related to the pyrimidine π system. These two (DTU) or three (2TU, 4TU) bands are well separated.

In the monosubstituted thiouracils (2TU and 4TU) the position of the substitution has some effect on the band shape. With reasonably good resolution in the energy domain, we predict that the two molecules could be discerned mainly by the shape of the bands that originate from ionization from the oxygen orbitals at around 10 eV binding energy. The photoelectron spectrum of DTU is easily distinguishable from that of the other compounds since it lacks the band from the oxygen-orbital ionization completely and in return it shows an intense double peak from the ionization out of orbitals located on the sulphur atoms.

An inspection of the excited-state photoelectron spectra from the S_1 and S_2 states of 2TU shows that the excited states can be detected without being disturbed by the ground state signal. Furthermore, the photoelectron spectra of 2TU simulated at the relevant S_1 and T_1 minima show strong overlap and very similar intensity. Hence, experimental pump-probe UV-TRPES using single-photon ionization alone might not be able to track the populations of the different excited singlet and triplet states and therefore intersystem crossing could be opaque to this methodology. However, other experimental techniques like multi-photon ionization might still be able to detect a signature from intersystem crossing.

ACKNOWLEDGMENTS

This work was financed by the Austrian Science Fund (FWF) Project No. P25827. Part of the calculations was performed on the Vienna Scientific Cluster 3 (VSC3). The authors want to thank Esther Heid for preliminary calculations, Susanne Ullrich and Carlos Crespo-Hernández for bringing up questions related to photoelectron spectra on thiouracils and the COST Action No. CM1204 (XLIC) for providing an environment for stimulating discussions. We also want to thank Serguei Patchkovskii and Michael Spanner for discussions and for providing their code for Dyson orbital calculations which helped our development very much.

[1]H. G. Zachau, Angew. Chem., Int. Ed. **8**, 711 (1969).
[2]M. N. Lipsett, J. Biol. Chem. **240**, 3975 (1965).
[3]A. Favre, C. Saintomé, J.-L. Fourrey, P. Clivio, and P. Laugâa, J. Photochem. Photobiol., B **42**, 109 (1998).
[4]A. Favre, "Thiouridine as an intrinsic photoaffinity probe of nucleic acid structure and interactions," in *Bioorganic Photochemistry, Photochemistry and the Nucleic Acids* (Wiley, 1990), Vol. 1 Chap. 4.
[5]O. Reelfs, P. Karran, and A. R. Young, Photochem. Photobiol. Sci. **11**, 148 (2012).
[6]A. Massey, Y. Z. Xu, and P. Karran, Curr. Biol. **11**, 1142 (2001).
[7]D. S. Cooper, N. Engl. J. Med. **352**, 905 (2005).
[8]N. Igarashi-Yamamoto, A. Tajiri, M. Hatano, S. Shibuya, and T. Ueda, Biochim. Biophys. Acta, Nucleic Acids Protein Synth. **656**, 1 (1981).
[9]M. Pollum, L. Martínez-Fernández, and C. E. Crespo-Hernández, in *Photoinduced Phenomena in Nucleic Acids I*, Topics in Current Chemistry Vol. 356, edited by M. Barbatti, A. C. Borin, and S. Ullrich (Springer, Berlin, Heidelberg, 2014), pp. 245–327.
[10]M. Pollum and C. E. Crespo-Hernández, J. Chem. Phys. **140**, 071101 (2014).
[11]G. Cui and W.-h. Fang, J. Chem. Phys. **138**, 044315 (2013).
[12]J. P. Gobbo and A. C. Borin, Comput. Theor. Chem. **1040-1041**, 195 (2014).
[13]S. Mai, P. Marquetand, and L. González, J. Phys. Chem. A **119**, 9524 (2015).
[14]L. Martínez-Fernández, L. González, and I. Corral, Chem. Commun. **48**, 2134 (2012).
[15]L. Martínez-Fernández, I. Corral, G. Granucci, and M. Persico, Chem. Sci. **5**, 1336 (2014).
[16]V. Vendrell-Criado, J. A. Saez, V. Lhiaubet-Vallet, M. C. Cuquerella, and M. A. Miranda, Photochem. Photobiol. Sci. **12**, 1460 (2013).
[17]M. Pollum, S. Jockusch, and C. E. Crespo-Hernández, J. Am. Chem. Soc. **136**, 17930 (2014).
[18]K. Taras-Goślińska, G. Burdziński, and G. Wenska, J. Photochem. Photobiol., A **275**, 89 (2014).
[19]M. Pollum, S. Jokusch, and C. Crespo-Hernández, Phys. Chem. Chem. Phys. **17**, 27851 (2015).
[20]H. Rostkowska, K. Szczepaniak, M. J. Nowak, J. Leszczynski, K. KuBulat, and W. B. Person, J. Am. Chem. Soc. **112**, 2147 (1990).
[21]C. Párkányi, C. Boniface, J.-J. Aaron, M. D. Gaye, R. Ghosh, L. von Szentpály, and K. S. RaghuVeer, Struct. Chem. **3**, 277 (1992).
[22]H. Moustafa, M. F. Shibl, and R. Hilal, Phosphorus, Sulfur Silicon Relat. Elem. **180**, 459 (2005).
[23]A. Khvorostov, L. Lapinski, H. Rostkowska, and M. J. Nowak, J. Phys. Chem. A **109**, 7700 (2005).
[24]O. Dolgounitcheva, V. G. Zakrzewski, and J. V. Ortiz, J. Chem. Phys. **134**, 074305 (2011).
[25]X. Li, J. Chen, and K. H. Bowen, J. Chem. Phys. **134**, 074304 (2011).
[26]A. R. Katritzky, M. Szafran, and G. Pfister-Guillouzo, J. Chem. Soc., Perkin Trans. 2 **1990**, 871.
[27]A. Stolow, A. E. Bragg, and D. M. Neumark, Chem. Rev. **104**, 1719 (2004).
[28]M. S. de Vries, *Photoinduced Phenomena in Nucleic Acids I*, Topics in Current Chemistry Vol. 355 (Springer, Berlin, Heidelberg, 2014), pp. 33–56.
[29]M. Schwell and M. Hochlaf, *Photoinduced Phenomena in Nucleic Acids I*, Topics in Current Chemistry Vol. 355 (Springer, Berlin, Heidelberg, 2014), pp. 155–208.
[30]B. McFarland, J. Farrell, S. Miyabe, F. Tarantelli, A. Aguilar, N. Berrah, C. Bostedt, J. Bozek, P. Bucksbaum, J. Castagna, R. Coffee, J. Cryan, L. Fang, R. Feifel, K. Gaffney, J. Glownia, T. Martinez, M. Mucke, B. Murphy, A. Natan, T. Osipov, V. Petrović, S. Schorb, T. Schultz, L. Spector, M. Swiggers, I. Tenney, S. Wang, J. White, W. White, and M. Gühr, Nat. Commun. **5**, 4235 (2014).
[31]S. Mai, M. Richter, P. Marquetand, and L. González, in *Photoinduced Phenomena in Nucleic Acids I*, Topics in Current Chemistry Vol. 355, edited by M. Barbatti, A. C. Borin, and S. Ullrich (Springer, Berlin, Heidelberg, 2014), pp. 99–153.
[32]A. Golan, K. B. Bravaya, R. Kudirka, O. Kostko, S. R. Leone, A. I. Krylov, and M. Ahmed, Nat. Chem. **4**, 323 (2012).
[33]J. C. Poully, J. P. Schermann, N. Nieuwjaer, F. Lecomte, G. Gregoire, C. Desfrancois, G. A. Garcia, L. Nahon, D. Nandi, L. Poisson, and M. Hochlaf, Phys. Chem. Chem. Phys. **12**, 3566 (2010).
[34]M. Spanner, S. Patchkovskii, C. Zhou, S. Matsika, M. Kotur, and T. C. Weinacht, Phys. Rev. A **86**, 053406 (2012).
[35]S. Gozem, A. O. Gunina, T. Ichino, D. L. Osborn, J. F. Stanton, and A. I. Krylov, J. Phys. Chem. Lett. **6**, 4532 (2015).
[36]H. R. Hudock, B. G. Levine, A. L. Thompson, H. Satzger, D. Townsend, N. Gador, S. Ullrich, A. Stolow, and T. J. Martínez, J. Phys. Chem. A **111**, 8500 (2007).
[37]H. R. Hudock and T. J. Martínez, ChemPhysChem **9**, 2486 (2008).
[38]H. Tao, T. Allison, T. Wright, A. Stooke, C. Khurmi, J. van Tilborg, Y. Liu, R. Falcone, A. Belkacem, and T. J. Martínez, J. Chem. Phys. **134**, 244306 (2011).
[39]C. M. Oana and A. I. Krylov, J. Chem. Phys. **127**, 234106 (2007).
[40]M. Spanner and S. Patchkovskii, Phys. Rev. A **80**, 063411 (2009).
[41]A. P. Thorne, in *Spectrophysics*, edited by A. P. Thorne (Springer, Netherlands, 1988).
[42]H. Lischka, T. Müller, P. G. Szalay, I. Shavitt, R. M. Pitzer, and R. Shepard, WIREs Comput. Mol. Sci. **1**, 191 (2011).
[43]H. Lischka, R. Shepard, I. Shavitt, R. M. Pitzer, M. Dallos, T. Müller, P. G. Szalay, F. B. Brown, R. Ahlrichs, H. J. Böhm, A. Chang, D. C. Comeau, R. Gdanitz, H. Dachsel, C. Ehrhardt, M. Ernzerhof, P. Höchtl, S. Irle, G. Kedziora, T. Kovar, V. Parasuk, M. J. M. Pepper, P. Scharf, H. Schiffer,

M. Schindler, M. Schüler, M. Seth, E. A. Stahlberg, J.-G. Zhao, S. Yabushita, Z. Zhang, M. Barbatti, S. Matsika, M. Schuurmann, D. R. Yarkony, S. R. Brozell, E. V. Beck, J.-P. Blaudeau, M. Ruckenbauer, B. Sellner, F. Plasser, and J. J. Szymczak, COLUMBUS, an *ab initio* electronic structure program, release 7.0, 2012.

[44]M. Reiher, WIREs Comput. Mol. Sci. **2**, 139 (2012).

[45]F. Aquilante, J. Autschbach, R. K. Carlson, L. F. Chibotaru, M. G. Delcey, L. De Vico, I. F. Galván, N. Ferré, L. M. Frutos, L. Gagliardi, M. Garavelli, A. Giussani, C. E. Hoyer, G. Li Manni, H. Lischka, D. Ma, P.-Å. Malmqvist, T. Müller, A. Nenov, M. Olivucci, T. B. Pedersen, D. Peng, F. Plasser, B. Pritchard, M. Reiher, I. Rivalta, I. Schapiro, J. Segarra-Martí, M. Stenrup, D. G. Truhlar, L. Ungur, A. Valentini, S. Vancoillie, V. Veryazov, V. P. Vysotskiy, O. Weingart, F. Zapata, and R. Lindh, J. Comput. Chem. **37**, 506 (2016).

[46]T. H. Dunning, Jr., J. Chem. Phys. **90**, 1007 (1989).

[47]D. E. Woon and T. H. Dunning, Jr., J. Chem. Phys. **98**, 1358 (1993).

[48]See supplementary material at http://dx.doi.org/10.1063/1.4941948 for an accuracy assessment of MRCIS, vertical ionization energies and Dyson norms at S_0 minima, geometry data and, active orbitals.

[49]F. Plasser, M. Ruckenbauer, S. Mai, M. Oppel, P. Marquetand, and L. González, "Efficient and flexible computation of many-electron wavefunction overlaps," J. Chem. Theory Comput. (published online).

[50]M. Richter, P. Marquetand, J. González-Vázquez, I. Sola, and L. González, J. Chem. Theory Comput. **7**, 1253 (2011).

[51]S. Mai, M. Richter, M. Ruckenbauer, M. Oppel, P. Marquetand, and L. González, Sharc: Surface hopping including arbitrary coupling—Program package for non-adiabatic dynamics, 2014, http://sharc-md.org.

[52]S. Mai, P. Marquetand, and L. González, Int. J. Quantum Chem. **115**, 1215 (2015).

[53]D. L. Yeager, in *Many-Body Methods in Quantum Chemistry*, edited by U. Kaldor (Springer-Verlag, Berlin, Heidelberg, 1988).

[54]R. J. Bartlett, Annu. Rev. Phys. Chem. **32**, 359 (1981).